JOURNAL OF INTEGRATED OMICS
A METHODOLOGICAL JOURNAL
HTTP://WWW.JIOMICS.COM

ORIGINAL ARTICLE | DOI: 10.5584/jiomics.v4i2.158

Characterization of temperature-sensing and PIP_2-regulation of TRPV1 ion channel at the C-terminal domain using NMR spectroscopy and Molecular Dynamics Simulations

Kelly A. Raymond[1], Edward C. Twomey[1,2,†], Yufeng Wei*[2]

[1]Department of Chemistry and Biochemistry, Seton Hall University, South Orange, NJ 07079-2694, USA; [2]Institute of NeuroImmune Pharmacology, Seton Hall University, South Orange, NJ 07079-2694, USA; [†]Current Address: Integrated Program in Cellular, Molecular, and Biomedical Studies, Columbia University, New York, NY 10032, USA.

Received: 14 November 2013 **Accepted:** 04 August 2014 **Available Online**: 30 September 2014

Abstract

Transient receptor potential (TRP) channels are receptors of stimulating signals, such as temperature, taste, odor, and chemo- and mechano-stimuli. Temperature sensing TRP channels coincidently function as pain receptors, and are potential targets for substances of abuse, including alcohol and illicit drugs. TRP vanilloid type 1 (TRPV1) channel is activated by heat (>43 °C) and capsaicin under the tight regulation of membrane-associated second messenger, PIP_2 (phosphatidylinositol-4,5-bisphosphate), responds to noxious stimuli and inflammatory substances, and could potentially modulate effects of alcohol and drugs of abuse. Despite the crucial roles in mediating signal transductions at both peripheral and central nervous systems, TRP channels are poorly understood in the context of structures and mechanisms. In this study, we describe our initial structural characterization of the TRPV1 C-terminal domain, the putative temperature sensing and PIP_2-regulatory domain, using NMR spectroscopy and molecular dynamics simulations. Both experimental and computational models suggest that the C-terminal domain is intrinsically unstructured at room temperature with and without lipid bicelles. Elevated temperature and PIP_2-binding can induce substantial conformational changes and formation of considerable secondary structural components in the C-terminal domain, which could be transduced to the transmembrane domain to potentially sensitize the channel.

Keywords: membrane protein; molecular dynamics; NMR; phospholipids; signal transduction; transient receptor potential channel.

Abbreviations

MD: molecular dynamics; **NMR**: nuclear magnetic resonance; **NOE**: nuclear Overhauser effect; **PIP_2**: phosphatidylinositol-4,5-bisphosphate; **TRP**: transient receptor potential.

1. Introduction

TRP channels are generally described as the vanguard of our sensory systems that respond to a variety of intra- and intercellular stimuli [1, 2]. The thermo TRP channels are activated by distinct physiological temperatures, and are involved in converting thermal information into chemical and electrical signals within the sensory nervous system. The homologously related TRPV1, TRPV2, TRPV3, and TRPV4 are activated by increased temperature, while TRPM8 and TRPA1, the more distinctly related TRP channels, are activated upon cooling [3, 4]. In addition to temperature, these channels can be activated by a number of agonists. For example, capsaicin, the pungent extract of hot peppers, can activate TRPV1; menthol, the cooling compound extracted from the mint plant, directly activates TRPM8; and mustard oil and cinnamaldehyde from the cinnamon oil specifically activate TRPA1 [2, 4].

***Corresponding author:** Yufeng Wei, Ph.D. Institute of NeuroImmune Pharmacology, Seton Hall University, 400 South Orange Ave, South Orange, NJ 07079-2694, USA; Phone: 973-275-2335; Fax: 973-761-9772; Email-Address: Yufeng.Wei@shu.edu

Coincidently, thermo TRP channels are receptors of noxious stimuli, leading to acute nociceptive pain, a protective warning of damage [5, 6]. However, many pathological conditions lead to changes in the expression level and/or sensitivity of nociceptive TRP channels, characterized as hyperesthesia. These pathological conditions include inflammations (inflammatory pain) and damage or lesions to the nervous system (neuropathic pain) [7]. Recent research also suggests that alcohol can modulate thermo TRP channel activities. TRPM8 activity is inhibited by high concentration of ethanol [8], while TRPV1 and TRPA1 are activated and potentiated by ethanol [9-11]. Using TRPV1 knockout mice, the roles of TRPV1 in the avoidance of the adverse alcohol taste and alcohol-induced intoxication were established [12, 13].

Most recently, high-resolution structures of TRPV1 ion channel were determined using state-of-the-art single particle cryo-electron microscopy (cryo-EM) technique [14], and distinct conformations were revealed upon activation of the channel [15]. These structures contains amazingly detailed information on the arrangement of the transmembrane segments, including the ion passage pore, and the cytosolic N-terminal domain, including the ankyrin repeats. However, the TRPV1 structure (PDB ID: 3J5P) was obtained using a minimal functional construct composed of residues 110-603 and 627-764 [14], which lacks about half of the cytosolic C-terminal domain (residues 684-839). In addition, this structure lacked electron density in the C-terminal region with the exceptions of the TRP domain α-helix and a β-strand close to the end of the minimal construct. This observation strongly suggested a largely unstructured C-terminal domain that could undergo significant conformational change upon activation or ligand binding.

The intrinsically disordered C-terminal domain of TRPV1 is functionally critical. It has been suggested that the cytosolic C-terminal domains of thermo TRPs are responsible for mediating TRP channel activities. Swapping mutageneses experiments indicated that the C-terminal domains of TRPV1 and TRPM8 determine the activation phenotype by temperature of these channels [16]. It is also determined that a region located outside the TRP domain comprising the TRPV1 C-terminal amino acids Q727 to W752 (corresponding TRPM8 C-terminal amino acids K1030 to W1055) is the minimal portion to show temperature sensitivity (heat or cold), and deletion of 11 residues, comprising of TRPV1 C741 to W752, results in losing channel thermal sensitivity while retaining voltage sensitivity [17]. The minimal construct used to obtain the TRPV1 structure contained this temperature-sensing segment (residues 727 – 752), and the minimal construct was reported to respond to heat [14].

PIP_2 (phosphatidylinositol-4, 5-bisphosphate) is an essential modulator for TRP channels, as well as a wide range of other ion channels [18]. PIP_2 activates TRPM8, and activation of phospholipase C (PLC) and subsequent depletion of PIP_2 desensitize the channel [19, 20]. On the other hand, TRPV1 is desensitized by PIP_2, and depletion of cellular PIP_2 upon activation of PLC activates TRPV1 [21]. However, the role of PIP_2 on TRPV1 modulation is still controversial, as experiments also show that PIP_2 sensitizes TRPV1 and that depletion leads to desensitization [22, 23]. A dual regulatory role is also suggested [24]. It has been suggested that the conserved positively charged clusters in the C-terminal domain of TRP channels are responsible for PIP_2 binding. The putative PIP_2 binding site for TRPM8 is on the very proximal C-terminal TRP domain (K995, R998, K1008) [20], whereas in TRPV1, it is located on the more distal C-terminal region after the TRP domain (R786, K789, R798) [21]. A homology model of TRPV1, built upon the crystal structures of Kv1.2 [25] and HCN2 [26] as templates for transmembrane and C-terminal regions, respectively, suggests that PIP_2 aliphatic chains are located near the voltage-sensor modules, while the PIP_2 polar head group is interacting with a cluster of positive charges located in the proximal C-terminal region, including residues K694, K698, K701, and K710, as well as with amino acids R575 and R579 located in the S4-S5 linker helix [27]. The C-terminal domain in this homology model, however, did not seem to agree with the recent cryo-EM structure, which indicated a mostly unstructured C-terminal domain with an α-helical TRP domain and a β-strand in the temperature sensor [14], while the homology model showed a mostly well-folded C-terminal domain with all helical components within the temperature sensor [27].

Thermo and nociceptive TRP channels have the ability to integrate multiple stimuli, and temperature activation thresholds can be shifted in response to algogenic substances, phospholipid signaling molecules, phosphorylation states, mild acidic conditions, and membrane voltage. A modular model with allosteric gating mechanism of thermo TRP channels was proposed to explain the TRP mechanisms [28]. Current *in vivo* studies on the functions of TRP channels involves mostly the use of transgenic mouse models, providing a productive source of validated targets for future drug discovery [29]. Nevertheless, mouse gene knockouts can be problematic pertaining to pain phenotyping. For example, thermo and pain reception can be compensated by related channels and receptors, and differences between mouse strains can be significant [30]. Moreover, the lack of knowledge on the detailed mechanisms and structures of TRP channels, particularly the C-terminal domain, severely hampers the ability to understand the mechanistic role of TRP channels in nociception and the development of drugs to target TRP channels [31]. TRPV1 is the only member of the TRP superfamily that has been targeted in the treatment of pain, bladder, and gastrointestinal diseases [32]. The minimal construct of the TRPV1 possessed the temperature-sensing segment (residues 727-752), but not the regulatory PIP_2/calmodulin binding segment (residues 778-819), suggesting that the temperature sensing and regulatory segments are functionally independent and structurally unrelated. Considering the intrinsically disordered nature of the C-terminal domain, we have studied these two segments as individual peptides in an initial attempt, and combined with molecular dynamics (MD) simulation of the full-length C-

terminal domain to integrate the findings of the individual peptides into a more complete model. Here we report our initial NMR spectroscopic characterization of the putative temperature-sensing and PIP_2-interacting segments of the C-terminal domain of TRPV1 channel at various conditions, complemented by an MD simulation of the complete C-terminal domain at two different temperatures.

2. Material and Methods

Peptide synthesis

The C-terminal segment that shows temperature sensitivity of human TRPV1 residues 727-752 with sequence QVGYTPDGKDDYRWCFRVDEVNWTTW and the putative PIP_2-interacting segment of human TRPV1 protein residues 778-819 with sequence of LRSGRVSGRNWKN FALVPLLRDASTRDRHSTQPEEVQLKHYT were synthesized and purified at the Proteomics Resource Center of the Rockefeller University, and their identities were confirmed by mass spectrometry.

NMR sample preparation

All NMR samples were prepared in 20 mM sodium phosphate buffer, pH 6.6, 150 mM NaCl, in 90%/10% H_2O/D_2O solvent. The phospholipids, DHPC, DMPC, DMPG, and brain PIP_2 were purchased from Avanti Polar Lipids, Inc. (Alabaster, AL). A 15% stock bicelle solution was formed at a molar ratio of 0.53 DHPC:0.27 DMPC:0.20 DMPG in the above buffer [33]. The hTRPV1 727-752 peptide (temperature sensor) was dissolved in the above buffer to a final concentration of 4.0 mg/ml. The mTRPV1 778-819 peptide (PIP_2 interacting segment) was prepared in the buffer and in the bicelle solution in the absence and presence of 4 mol% brain PIP_2. The final peptide concentration in all samples was 3.3 mg/ml and final lipid concentration was 5%.

NMR spectroscopy

All NMR spectra were acquired on a Bruker Avance 900 MHz spectrometer, equipped with a cryogenically cooled TCI-probe, operating at a ^1H frequency of 900.154 MHz. Standard two-dimensional NOESY pulse sequence was used for samples without lipid bicelles, and a ω_2-selective NOESY pulse sequence, in which the final excitation pulse was replaced by an E-BURP2 pulse selective for the frequency region of 6.5 – 10.5 ppm, was used for samples containing lipid bicelles [34]. The NOESY mixing times were set to 100, 200, and 300 ms. 4096×1024 complex data points were collected in each experiment with spectral widths of 11682.243 Hz (or 12.978 ppm) in both dimensions. 16 transients were collected for each 2D increment. The experiments were performed at 25, 35, and 45 °C (298, 308, and 318 K). All spectra were processed using NMRPipe [35], and analyzed and displayed using NMRViewJ [36].

Molecular dynamics simulations

A BLAST search indicated that two proteins are structurally homologous to human TRPV1 C-terminal domain, G684-K839, with PDB ID 2HE7 [37] homologous to the proximal end with sequence identity of 27/109 (25%), similarity of 41/109 (37%), and E-value of 1.3, and 2R5K [38] homologous to the distal end with sequence identity of 19/65 (29%), similarity of 30/65 (46%), and E-value of 4.3. A homology model was built upon these two proteins using program Modeller version 9.11 [39]. The homology model was then minimized and equilibrated using molecular dynamics simulation package NAMD version 2.9 [6] at 298 K and 318 K, respectively. The trajectories were simulated for 10 ns at 2 fs time step using periodic boundary conditions for water solvent under constant temperature/pressure and variable volume conditions. The restart frequency was set to 1 ps (every 500 steps) in the simulations. The structural equilibrations were assessed using graphical presentation tool VMD version 1.91 [40] and the structures were visualized using PyMOL version 1.5 (http://www.pymol.org/).

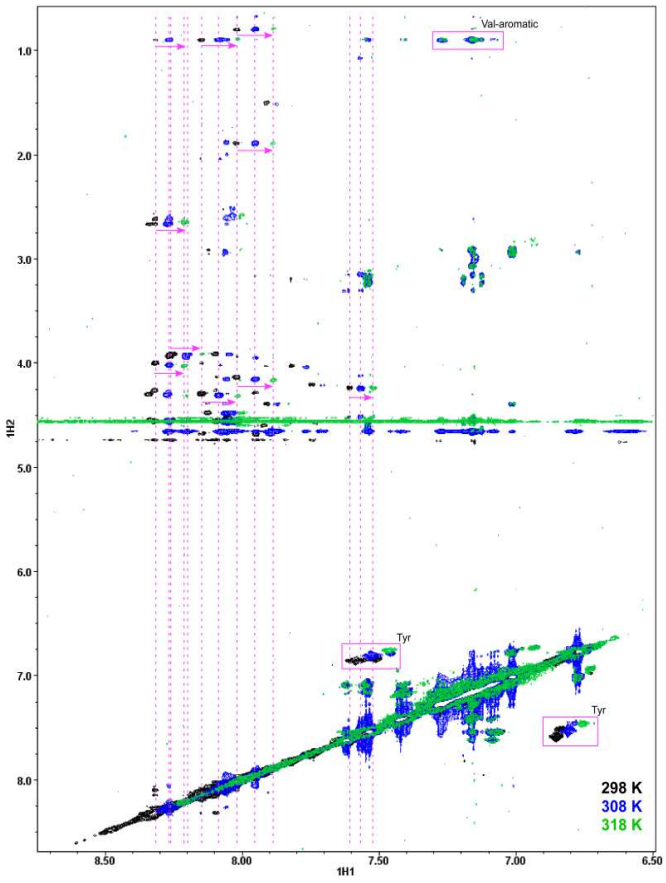

Figure 1. Overlaid NOESY spectra of human TRPV1 residues Q727-W752, the putative temperature sensing segment, at temperatures of 25, 35, and 45 ˚C. The arrows indicate resonance shift of all three valine residues upon increase in temperature, and boxes highlight aromatic-valine interactions and shifts in Tyr resonances in response to temperature change.

3. Results

3.1 *NMR spectroscopy of TRPV1 temperature-sensing segment (Q727-W752)*

The 300-ms mixing time NOESY spectra (amide-aromatic region) of the hTRPV1 temperature-sensing segment, residues Q727-W752, at different temperatures (298, 308, and 318 K) are shown in Figure 1. This segment displays extended, strand-like, secondary structural feature, with inter-chain N-H/N-H (d_{NN}) NOE cross peaks observed at room temperature. Upon increase in temperature, the three valine residues exhibit the most significant shifts, while the single tyrosine residue also shifts continuously. New interactions between valine methyl groups and aromatic residues are appearing only at elevated temperatures (308 and 318 K), whereas the inter-chain d_{NN} NOE cross peaks are disappearing at high temperatures. These observations indicate that upon increase in temperature, the temperature sensing segment experiences significant conformational change, and the hydrophobic core interactions are reorganizing in response to temperature change. The conformational changes at the temperature sensing segment are likely transferred to the transmembrane domain under the regulation at the PIP_2 binding segment.

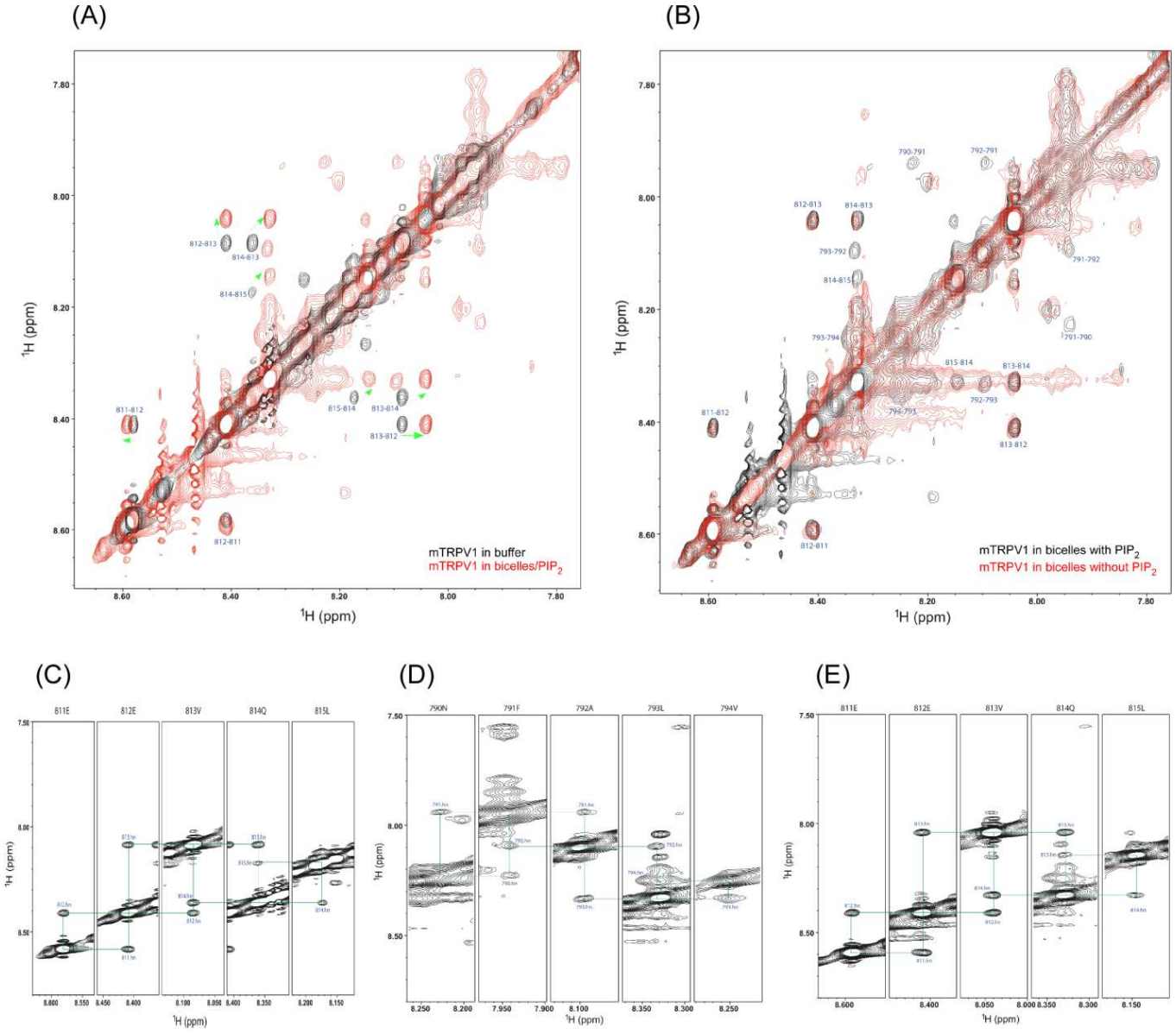

Figure 2. NOESY spectra of mTRPV1 778-819 peptide. (A) Overlay of the d_{NN} region of the peptide in buffer and in lipid bicelles with PIP_2; (B) Overlay of the d_{NN} region of the peptide in lipid bicelles with and without PIP_2; (C) d_{NN} connectivity of the helical stretch 811-815 without bicelles/PIP_2; (D) d_{NN} connectivity of the helical stretch 790-794 in lipid bicelles with PIP_2; (E) d_{NN} connectivity of the helical stretch 811-815 in lipid bicelles with PIP_2.

3.2 *NMR spectroscopy of TRPV1 PIP_2-binding segment (residues L778-T819)*

The hTRPV1 PIP_2-interacting peptide is largely unstructured in phosphate buffer without lipids in the temperature range of 25-45 ˚C, with the exception of a short stretch of residues 811-815, where a helical structure is evidenced by the sequential d_{NN} NOEs (Figure 2A and C). In the presence of lipid bicelles (0.53 DHPC: 0.27 DMPC: 0.20 DMPG), however, the hTRPV1 peptide undergoes significant conformational change, and a great number of helical elements can be observed by dNN NOEs, especially when PIP_2 is present (Figure 2B, D, and E). Although the helical stretch of 811-815 is retained both in phosphate buffer and in lipid bicelles, the resonances have shifted significantly (Figure 2A), indicating a completely different environment experienced by the helix. Comparing the spectra of hTRPV1 in bicelles with and without PIP_2 (Figure 2B), many peaks are broadened in the hTRPV1 spectrum when PIP_2 is absent, indicating an intermediate exchange between the lipid bicelles and hTRPV1 peptide, while these peaks are clearly visible when PIP_2 is present in the sample, suggesting a reinforced interaction between the peptide and PIP_2. The broadened peaks in the absence of PIP_2 mostly come from the helical stretch of 790-794, situated in the middle of the key residues R786, K789, and R798, suggesting an essential roles of these residues in mediating PIP_2 interaction through an induced conformational change in this region.

3.3 *Molecular dynamics simulations of TRPV1 C-terminal domain*

A homology model for human TRPV1 C-terminal domain, residues G684-K839, was built from 2HE7 (FERM domain of EPB41L3) and 2R5K (Pentamer Structure of Major Capsid protein L1 of Human Papilloma Virus type 11) structures that cover the full sequence of TRPV1 C-terminal domain. The sequence alignment between TRPV1 C-terminal domain and 2HE7 and 2R5K sequences is illustrated in Figure 3. Five homology structures were generated by Modeller program [39], and the model with lowest objective function (molpdf) value and DOPE assessment score was selected for additional molecular dynamics simulations using NAMD package at 298 and 318 K, respectively. The MD models at both temperatures were properly equilibrated over 10 ns simulations, as indicated by the absence of vacuum holes between identical periodic images and small changes in volume over time of the simulated structures.

Although there is a homology model of the full length TRPV1 [27], the validity of this model is questionable. This model showed a mostly structured C-terminal domain, while the most recent experimental structure suggested a disordered domain. In addition, our experimental results do not support the C-terminal domain features reported in the model. The most discrepancy lies in the temperature sensor: our data indicates an extended secondary structure, which was confirmed by a β-strand observed in the cryo-EM structure, while the model suggested a helical structure for the same region. Our models for the TRPV1 C-terminal domain, shown in Figure 4, are, in general, consistent with the NMR experimental data, and are complementary to the cryo-EM experimental structure with limited information on the C-terminal domain. Our model structures at both temperatures show two helices at the proximal C-terminal domain, consisting of the conserved TRP box and the TRP domain that would link to the putative transmembrane segment. These two helices represent the coiled-coil domain, and are responsible for channel oligomerization. Down to the distal part of the C-terminal domain, both the temperature sensor (residues 727 -752, green) and the regulatory PIP_2-binding segment (residues 778 – 819, blue) are largely unstructured, with the exception of a short stretch of a-helix in the PIP_2-binding segment (Figure 4A). At room temperature (25 ˚C), the non-polar residues within the temperature sensor (grey, space filled) are not close to each other in three-dimensional space. At channel activating temperature (45 ˚C), the non-polar residues in the temperature sensor reorganize to form a hydrophobic core, consistent with NMR data that shows the appearance of NOE cross peaks between aromatic and valine residues. The formation of the hydrophobic core induces conformational change in the heat sensor, and extended antiparallel β-sheets are formed. At elevated temperature, additional conformational changes are also observed in the regulatory PIP_2-binding segment as the conformation becomes more extended in this region and a short stretch of helix also forms (Figure 4B). In addition, the coiled-coil

```
2HE7      257  PNHTKELEDKVIELHKSHRGMTPAEAEMHFLENAKKLSMYGVDLHHAKDSEGVEIMLGVC
hTRPV1    684  GETVNKIAQESKNIWKLQRAITILDTEKSFLKCMRKA-----------FRSGKLLQVGYT
2R5K              ------------------------------------------------------------

2HE7      317  ASGLLIYRDRLRINRFAWPKVLKISYKRNNFYIKIRPGEFEQFESTIGFKLPNHRAAKRL
hTRPV1    733  PDGKDDYRWCFRVDEVNWTT-----WNTNVGIINEDPGNCEGVKRTLSFSLRSSRVSGRH
2R5K      225  ----------------------------------------------LFFYLRKEQMFARH

2HE7      377  WK----------------------------------------------------------
hTRPV1    788  WKNFAL-----VPLLREASARDRQSAQPEEVYLRQFSGSLKPEDAEVFKSPAASGEK
2R5K      239  FFNRAGTVGEPVPDDLLVKGGNNRSSVASSIYVHTPSGSLVSSEAQLFNKP------
```

Figure 3. Sequence alignment of human TRPV1 C-terminal domain (residues 684-839) with PDB files 2HE7 and 2R5K. Identical residues are shaded black and similar residues are shaded grey. The alignment E-values are 1.3 for 2HE7 and 4.3 for 2R5K.

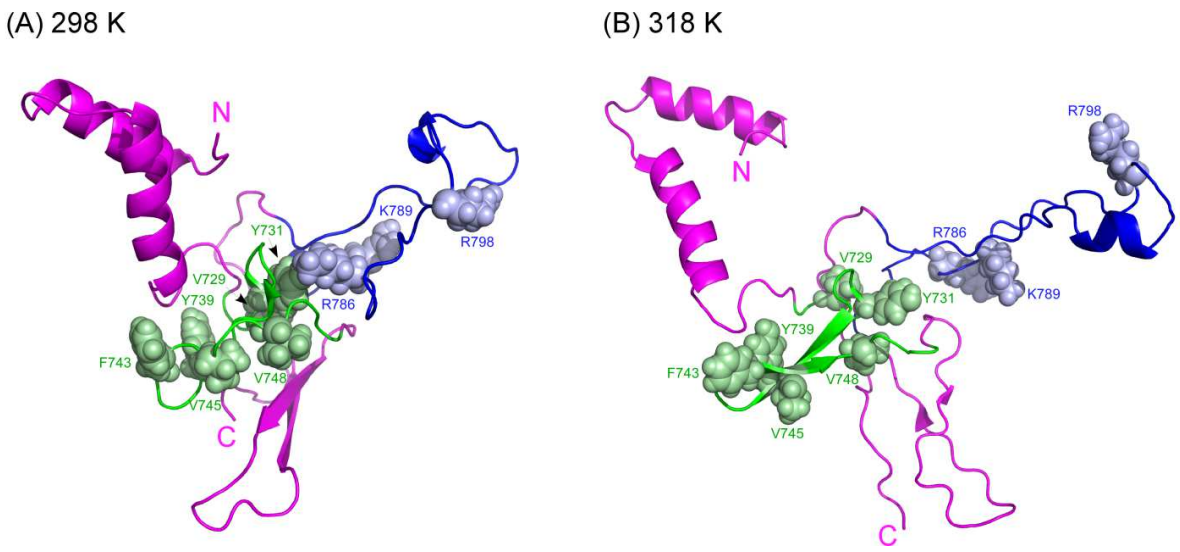

Figure 4. Computational models of TRPV1 C-terminal domain (residues 684-839) at 298 K (A) and 318 K (B). The temperature sensor (727 – 752) is colored green, and the regulatory PIP_2-binding segment (778 – 819) is blue. The key residues forming the hydrophobic core (pale green) in the temperature sensor and the residues essential for PIP_2 binding (light blue) in the regulatory segment are shown as space-filling model.

structure along the TRP box and TRP domain changes the relative orientations between the two helices, indicating a conformational change migrating from the temperature sensor into the transmembrane segment.

4. Discussion

Temperature sensing TRP channels are modular, allosterically controlled, multifunctional protein sensors that can integrate a wide variety of stimuli, including temperature, acidic pH, cell membrane voltage, and intracellular Ca^{2+} levels, respond to chemical agonists, alcohols, and endogenous cannabinoids, and induce hyperesthesia under nociceptive, inflammatory, and neuropathic conditions. The functions and responses of TRP channels are also strictly regulated by membrane-associated second messengers (such as PIP_2) and phosphorylation states. Therefore, it is important to characterize the structures and conformations of the C-terminal domain in response to temperature and PIP_2 regulation, key information currently lacking from the literature. This study reports our initial attempt in obtaining structural information and assessing conformational changes of the TRPV1 C-terminal domain at atomic details under channel activating conditions.

At room temperature, both our NMR spectra and molecular dynamics (MD) model show that most regions of the C-terminal domain, including the heat sensor and PIP_2-regulatory segments, appear unstructured with the exception of two helices around the conserved TRP box and TRP domain, a coiled-coil segment responsible for the oligomerization of TRPV1 channel, consistent with the recent cryo-EM structure of TRPV1 showing an α-helical TRP domain [14]. At channel activating temperature (45 ˚C), our NMR experimental data and the MD model demonstrated a dramatic conformational change at the heat sensor, involving the formation of various hydrophobic valine-aromatic interactions, accompanied by increasing in the β-strand components in this segment. This C-terminal β-strand component was also observed in the cryo-EM structure [14], which is an important interaction point to the N-terminal domain. This change of conformation at the heat sensor propagates throughout the C-terminal domain, including the PIP_2-interacting segment and the coiled-coil structural motif, and eventually activates the channel and opens the pore in the transmembrane segment.

Our experimental NMR results, consistent with our MD models, also show that the TRPV1 PIP_2-interacting segment is intrinsically unstructured in the temperature range of 25-45 ˚C; only a short stretch of helical structure in this segment was revealed in the MD model, which was also observed in the NMR experiments. The TRPV1 PIP_2-binding segment seemed to be able to interact with the lipid bicelles, which consists of 80% neutral lipids (DHPC and DMPC) and 20% negatively charged lipids (DMPG). The TRPV1 C-terminal domain contains several clusters of basic residues (Lys and Arg) that are positively charged under experimental conditions (pH 6.6), including a segment near the TRP box and TRP domain (residues 694-721) and the putative PIP_2-interacting segment (residues 778-819). These positively charged basic residue patches may possibly interact with the negatively charged DMPG lipid through electrostatic interactions, but such interactions are largely non-specific, as evidenced by the broadened NOE cross peaks in the presence of lipid bicelles without PIP_2 (Figure 2B). Only in the presence of 4% PIP_2 (-4 charge under experimental conditions) in the lipid bicelles, the PIP_2-interacting segment undergoes significant conformational changes, clearly adopting secondary structures, as illustrated by the shifts and appear-

ance of new NOE cross peaks (Figure 2B). We believe that the PIP_2-interacting segment is involved in a specific, electrostatic interaction with the PIP_2 molecule. This observation agrees with early studies on other PIP_2-binding peptides (such as MARCKS) that these basic membrane-bound peptides only sequester multivalent (such as PIP_2), but not monovalent (such as PG or PS) acidic lipids [41, 42].

5. Concluding Remarks

TRPV1, a multifunctional ion channel protein, is an important drug target for novel analgesics and potential modulators of the effects of substances of abuse, including alcohol and illicit drugs. However, the lack of essential structural information on TRP channels greatly limits the understanding of the channel functions and mechanisms in mediating relevant biological processes and physiological effects. Here we report our experimental NMR studies and MD simulations in revealing potential structure-activity relationship of the TRPV1 C-terminal domain. In conclusion, the C-terminal domain is largely unstructured under normal conditions (25 ˚C), with the exception of the proximal TRP box and TRP domain region, which forms a helical coiled-coil structure, and is responsible for the oligomerization of the channel. At channel activating temperature (45 ˚C), the temperature sensor (residues 727 – 752) adopts an extended secondary structure with the formation of a hydrophobic core involving several valine and aromatic residues within the sensor. The structural changes at the temperature sensor induce a substantial conformational change throughout the C-terminal domain, and transmit into the transmembrane segment to activate the channel. The PIP_2-interacting segment (residues 778 – 819) is also intrinsically unstructured, although a short stretch of α-helix was observed. This segment specifically interacts with PIP_2 (-4 charge) electrostatically through clusters of basic residues, but does not interact with monovalent lipid, such as DMPG used in this study or POPS as in the actual mammalian plasma membrane. Our study confirms the important roles of the C-terminal domain in temperature sensing and PIP_2-regulation of the TRPV1 channel functions, and provides structural insights into the mechanisms of the C-terminal domain in mediating these stimuli. Although a high-resolution cryo-EM structure of a minimum TRPV1 construct is now available, this structure lacked the regulatory PIP_2-binding segment of the C-terminal domain, and besides the α-helix of the TRP domain and a β-strand within the temperature sensor, limited information was available for the functionally critical C-terminal domain in this experimental structure. Our models of the full C-terminal domain, complementary to the experimental structure, therefore, provide key information in understanding the channel functions.

Acknowledgements

We thank Proteomics Resource Center of the Rockefeller University for syntheses and characterizations of TRPV1 peptides, and the New York Structural Biology Center for high field NMR instrument time. We are also grateful for various funding and fellowships from the Eric F. Ross Research Foundation, Independent College Fund of New Jersey, New Jersey Space Grant Consortium/NASA, and University Research Council of Seton Hall University.

References

[1] D.E. Clapham, Nature, 426 (2003) 517-524. doi: 10.1038/nature02196

[2] T. Voets, K. Talavera, G. Owsianik, B. Nilius, Nature chemical biology, 1 (2005) 85-92. doi: 10.1038/nchembio0705-85

[3] A. Patapoutian, A.M. Peier, G.M. Story, V. Viswanath, Nature reviews. Neuroscience, 4 (2003) 529-539. doi: 10.1038/nrn1141

[4] M. Bandell, L.J. Macpherson, A. Patapoutian, Current opinion in neurobiology, 17 (2007) 490-497. doi: 10.1016/j.conb.2007.07.014

[5] D.N. Cortright, A. Szallasi, Current pharmaceutical design, 15 (2009) 1736-1749. doi: 10.2174/138161209788186308

[6] J.C. Phillips, R. Braun, W. Wang, J. Gumbart, E. Tajkhorshid, E. Villa, C. Chipot, R.D. Skeel, L. Kale, K. Schulten, J Comput Chem, 26 (2005) 1781-1802. doi: 10.1002/jcc.20289

[7] A. Patapoutian, S. Tate, C.J. Woolf, Nat Rev Drug Discov, 8 (2009) 55-68. doi: 10.1038/nrd2757

[8] J. Benedikt, J. Teisinger, L. Vyklicky, V. Vlachova, Journal of neurochemistry, 100 (2007) 211-224. doi: 10.1111/j.1471-4159.2006.04192.x

[9] J.A. Matta, P.M. Cornett, R.L. Miyares, K. Abe, N. Sahibzada, G.P. Ahern, Proceedings of the National Academy of Sciences of the United States of America, 105 (2008) 8784-8789. doi: 10.1073/pnas.0711038105

[10] M. Trevisani, D. Smart, M.J. Gunthorpe, M. Tognetto, M. Barbieri, B. Campi, S. Amadesi, J. Gray, J.C. Jerman, S.J. Brough, D. Owen, G.D. Smith, A.D. Randall, S. Harrison, A. Bianchi, J.B. Davis, P. Geppetti, Nature neuroscience, 5 (2002) 546-551. doi: 10.1038/nn852

[11] P.M. Cornett, J.A. Matta, G.P. Ahern, Molecular pharmacology, 74 (2008) 1261-1268. doi: 10.1124/mol.108.049684

[12] J.M. Ellingson, B.C. Silbaugh, S.M. Brasser, Behavior genetics, 39 (2009) 62-72. doi: 10.1007/s10519-008-9232-1

[13] Y.A. Blednov, R.A. Harris, Neuropharmacology, 56 (2009) 814-820. doi: 10.1016/j.neuropharm.2009.01.007

[14] M. Liao, E. Cao, D. Julius, Y. Cheng, Nature, 504 (2013) 107-112. doi: 10.1038/nature12822

[15] E. Cao, M. Liao, Y. Cheng, D. Julius, Nature, 504 (2013) 113-118. doi: 10.1038/nature12823

[16] S. Brauchi, G. Orta, M. Salazar, E. Rosenmann, R. Latorre, The Journal of neuroscience : the official journal of the Society for Neuroscience, 26 (2006) 4835-4840. doi: 10.1523/JNEUROSCI.5080-05.2006

[17] S. Brauchi, G. Orta, C. Mascayano, M. Salazar, N. Raddatz, H. Urbina, E. Rosenmann, F. Gonzalez-Nilo, R. Latorre, Proceedings of the National Academy of Sciences of the United States of America, 104 (2007) 10246-10251. doi: 10.1073/

pnas.0703420104

[18] B.C. Suh, B. Hille, Current opinion in neurobiology, 15 (2005) 370-378. doi: 10.1016/j.conb.2005.05.005

[19] B. Liu, F. Qin, The Journal of neuroscience : the official journal of the Society for Neuroscience, 25 (2005) 1674-1681. doi: 10.1523/JNEUROSCI.3632-04.2005

[20] T. Rohacs, C.M.B. Lopes, I. Michailidis, D.E. Logothetis, Nature neuroscience, 8 (2005) 626-634

[21] E.D. Prescott, D. Julius, Science, 300 (2003) 1284-1288. doi: 10.1126/science.1083646

[22] B. Liu, C. Zhang, F. Qin, The Journal of neuroscience : the official journal of the Society for Neuroscience, 25 (2005) 4835 -4843. doi: 10.1523/JNEUROSCI.1296-05.2005

[23] A.T. Stein, C.A. Ufret-Vincenty, L. Hua, L.F. Santana, S.E. Gordon, The Journal of general physiology, 128 (2006) 509-522. doi: 10.1085/jgp.200609576

[24] V. Lukacs, B. Thyagarajan, P. Varnai, A. Balla, T. Balla, T. Rohacs, The Journal of neuroscience : the official journal of the Society for Neuroscience, 27 (2007) 7070-7080. doi: 10.1523/JNEUROSCI.1866-07.2007

[25] S.B. Long, E.B. Campbell, R. Mackinnon, Science, 309 (2005) 897-903. doi: 10.1126/science.1116269

[26] W.N. Zagotta, N.B. Olivier, K.D. Black, E.C. Young, R. Olson, E. Gouaux, Nature, 425 (2003) 200-205. doi: 10.1038/nature01922

[27] G. Fernandez-Ballester, A. Ferrer-Montiel, The Journal of membrane biology, 223 (2008) 161-172. doi: 10.1007/s00232-008-9123-7

[28] R. Latorre, S. Brauchi, G. Orta, C. Zaelzer, G. Vargas, Cell calcium, 42 (2007) 427-438. doi: 10.1016/j.ceca.2007.04.004

[29] B.P. Zambrowicz, A.T. Sands, Nat Rev Drug Discov, 2 (2003) 38-51. doi: 10.1038/nrd987

[30] J.P. Hatcher, I.P. Chessell, Current opinion in investigational drugs, 7 (2006) 647-652

[31] R. Latorre, C. Zaelzer, S. Brauchi, Quarterly reviews of biophysics, 42 (2009) 201-246. doi: 10.1017/S0033583509990072

[32] A. Szallasi, D.N. Cortright, C.A. Blum, S.R. Eid, Nat Rev Drug Discov, 6 (2007) 357-372. doi: 10.1038/nrd2280

[33] J.F. Ellena, M.C. Burnitz, D.S. Cafiso, Biophysical journal, 85 (2003) 2442-2448. doi: 10.1016/S0006-3495(03)74667-0

[34] M. Seigneuret, D. Levy, Journal of biomolecular NMR, 5 (1995) 345-352. doi: 10.1007/BF00182276

[35] F. Delaglio, S. Grzesiek, G.W. Vuister, G. Zhu, J. Pfeifer, A. Bax, Journal of biomolecular NMR, 6 (1995) 277-293. doi: 10.1007/bf00197809

[36] B.A. Johnson, R.A. Blevins, Journal of biomolecular NMR, 4 (1994) 603-614. doi: 10.1007/BF00404272

[37] R.D. Busam, A.G. Thorsell, A. Flores, M. Hammarstrom, C. Persson, B. Obrink, B.M. Hallberg, The Journal of biological chemistry, 286 (2011) 4511-4516. doi: 10.1074/jbc.M110.174011

[38] B. Bishop, J. Dasgupta, M. Klein, R.L. Garcea, N.D. Christensen, R. Zhao, X.S. Chen, The Journal of biological chemistry, 282 (2007) 31803-31811. doi: 10.1074/jbc.M706380200

[39] A. Fiser, A. Sali, Charles W. Carter, Jr., M.S. Robert, Modeller: Generation and Refinement of Homology-Based Protein Structure Models, in: Methods in Enzymology, Academic Press, 2003, pp. 461-491.

[40] W. Humphrey, A. Dalke, K. Schulten, J Mol Graph, 14 (1996) 33-38, 27-38. doi: 10.1016/0263-7855(96)00018-5

[41] U. Golebiewska, A. Gambhir, G. Hangyas-Mihalyne, I. Zaitseva, J. Radler, S. McLaughlin, Biophysical journal, 91 (2006) 588-599. doi: 10.1529/biophysj.106.081562

[42] S. McLaughlin, D. Murray, Nature, 438 (2005) 605-611. doi: 10.1038/nature04398